Materials Transactions, Vol. 55, No. 9 (2014) pp. 1405 to 1413

Effect of Homogenization Treatment on the Microstructure and Mechanical Property Evolutions of As-Cast Al–Cu Alloy during High-Pressure Torsion

Mohamed Ibrahim Abd El Aal[1,2], Ho Yong Um[2], Kang Hyun Choi[2] and Hyoung Seop Kim[2]

[1]*Mechanical Design and Production Department, Faculty of Engineering, Zagazig University, Zagazig, Egypt*
[2]*Department of Material Science and Engineering, Pohang University of Science and Technology (POSTECH), Pohang 790-784, South Korea*

As-cast and homogenization treated as-cast Al–Cu (3 mass% Cu) alloy samples were processed via high-pressure torsion (HPT) under an applied pressure of 8 GPa with 5 revolutions at room temperature. Microstructure, mechanical properties, and fracture surface morphology of the HPT-processed Al–Cu were investigated, demonstrating that the HPT process successfully resulted in distinct grain refinements in both samples. Significant improvements in the microhardness, tensile properties, and deformation homogeneity due to fine grains, high grain boundary misorientation angle, and homogeneous distribution of the θ phase were achieved after the HPT process of the homogenized sample. The homogenization treatment of the as-cast Al–Cu has a significant effect on the fracture surface morphology and fracture mode of the HPT-processed samples. [doi:10.2320/matertrans.M2014047]

(Received February 17, 2014; Accepted June 6, 2014; Published July 18, 2014)

Keywords: *high-pressure torsion, ultrafine grained materials, aluminium–copper alloy, homogenization treatment*

1. Introduction

Recently, metallic ultrafine grained (UFG) materials defined as materials with nanometer or submicrometer grain sizes have received a great interest because of their unusual mechanical properties and high performance. One of the attractive techniques developed for producing bulk UFG metallic materials is severe plastic deformation (SPD),[1–4] such as high-pressure torsion (HPT),[5,6] equal channel angular pressing (ECAP),[7] and accumulative roll bonding.[8]

Al–Cu alloys are considered as very important structural materials in the aircraft industry due to their light weight and high strength.[9–13] Hence, the production of Al–Cu alloys with UFG microstructures, which leads to a significant improvement in the mechanical properties, was the main issue of research in the past decade. The microstructure, hardness, tensile properties, and fracture modes of Al-1.7, 0.63, and 3.9 mass% Cu alloys after ECAP were extensively studied.[14,15] Prados *et al.* studied the tensile behavior and fracture characteristics of the ECAP-processed Al-4 mass% Cu alloy.[16] The microstructure evolution, fracture characteristics, and the wear properties of the ECAP-processed Al-2, 3, and 5 mass% Cu alloys were also investigated.[17–19]

The effect of the homogenization treatment of the Al-2 and 3 mass% Cu alloys on the microstructural evolution, mechanical properties, fracture characteristics, and wear properties during the ECAP process was investigated;[20,21] and it was observed that the initial microstructure has an distinct effect on the grain refinement and mechanical properties during the ECAP process. Vafei *et al.*[22] reported the effect of pre- and post-heat treatments on the mechanical (hardness and torque) behaviors of the nano-grained Al-2024 alloy after the HPT process. Indeed, previous reports indicated that the initial microstructure affects the degree of the grain refinement during SPD and the mechanical properties of the ECAP-processed Al–Cu alloys.[20,21] However, there was no study on the effects of initial microstructure or homogenization heat treatment of as-cast Al–Cu alloys on the tensile testing and fracture behavior after the HPT process, as far as the authors know.

In this paper, the effect of the homogenization heat treatment of as-cast Al–Cu alloys on the microstructural evolution during and mechanical properties after the HPT process was investigated.

2. Experimental Procedure

Commercial purity aluminum and copper with a purity of 99.95 mass% were alloyed and sand cast in order to obtain the required Al-3 mass% Cu alloy. The as-cast Al–Cu alloy samples were homogenized at 550°C for 7 days (termed as homogenized samples). The as-cast and the homogenized samples were machined to disc-shaped samples with a 10 mm diameter and 2 mm thickness. Then, the samples were mechanically ground with No. 4000 SiC emery papers.

The shapes of the sample before and after the HPT process are presented in Fig. 1. The HPT process with 5 revolutions was performed at room temperature and a speed of 1 rpm under 8 GPa using a semi-constrained HPT die[3,5,6] with a 1 mm total depth and a 10 mm diameter.

The microstructure observations were performed before and after the HPT process. The microstructures of the as-cast and homogenized samples before the HPT process were investigated using an optical microscope in previous work.[20] A field emission scanning electron microscope (FE-SEM; model JEOL JSM-6330F, JEOL, Japan) operated at a voltage of 15 keV was used in the tracing of the fragmentation, distribution, and the size of theta phase θ ($CuAl_2$) after the HPT process. Moreover, the energy-dispersive X-ray spectroscopy (EDX) analysis of phase θ ($CuAl_2$) was performed using the same microscope. The average size of the θ phase was measured using the line intercept method and the image analysis software Lince242udt_particle size.

The ultrafine grains of as-cast and homogenized Al–Cu alloy samples after the HPT process were investigated using a transmission electron microscopy (TEM). The TEM samples were prepared through grinding with No. 4000 SiC emery

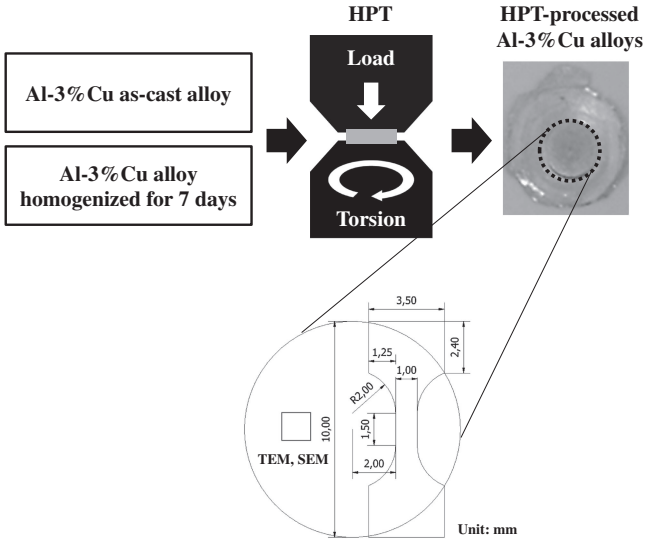

Fig. 1 Macrograph of Al-3%Cu as-cast and homogenized samples before and after HPT process and the positions of the TEM and SEM observations and tensile test sample.

papers, followed by mechanical polishing with alcohol and diamond paste suspensions to obtain mirror-like surfaces. The samples were further polished using mixtures of colloidal silica and ethanol for one hour in order to obtain a flat and shiny polished surface with a final thickness of 150 μm. Then, disc-shaped samples with a diameter of 3 mm were punched from the area in the mid-radius distance (2.5 mm from the HPT sample center), as indicated in Fig. 1, and then electro-polished using a solution of 30% HNO_3 + 70% CH_3OH. The fine microstructural observations were performed using the CS corrected field emission TEM microscope (JEOL JEM-2100F, Japan) operated at 200 KeV. The finest aperture size from which the selected-area electron diffraction (SAED) pattern can be taken was 10 μm. The average grain sizes of the HPT processed samples were obtained from the analysis the TEM photo-micrographs using the image analysis software Lince242udt_particle size.

The samples before and after the HPT process were carefully ground and polished to a mirror-like surface. The hardness was measured using a Mitutoyo microhardness tester equipped with a Vickers indenter under an applied load of 100 gf and a dwell time of 15 s. The measurements were recorded on the surface of each disk following a regular grid pattern with a spacing of 0.5 mm between each point.[23] The individual values of the Vickers hardness HV were then plotted as color-coded contour maps depicting the variations in the local microhardness across the surface of each sample. A total of 317 measurements was made across the sample and their average value was taken. The standard deviation σ of the 317 measurements was calculated in order to assess the deformation inhomogeneity index of the HPT processed samples using the following equation.

$$\sigma = \sqrt{\frac{\Sigma(H_i - H_{av})^2}{N}}, \quad (1)$$

where H_i, H_{av}, and N denote the microhardness value at each point of measurement, the average microhardness of the whole set of points of measurement, and the total number of measurements, respectively.

Microtensile testing for the HPT-processed samples was conducted at room temperature until failure using a UNITECH Microload system machine operated at a constant strain rate of $8.33 \times 10^{-3}\,s^{-1}$. Microtensile testing samples of a dog bone shape with 1.5 mm gage length were cut from the area in the mid-radius distance (2.5 mm from the HPT sample center) of the sample as shown in Fig. 1. The tensile samples were cut using a wire cutter followed by polishing of both sides of the sample to mirror-like surfaces. The tensile test was repeated three times for each condition. The fracture surface morphology and fracture mode of the tensile samples were examined using a field emission scanning electron microscope (FE-SEM, model JEOL JSM-6330F, Japan) at a voltage of 15 keV.

3. Results and Discussion

3.1 Microstructure of the Al–Cu alloy

The microstructures of the as-cast and the homogenized Al–Cu alloy samples before the HPT process were presented in previous works.[20] It was observed that the microstructure of the as-cast sample consists of dendrites with an average grain size of 113 ± 2 μm. After the homogenization treatment, most of the dendritic structures in the as-cast sample were transformed into approximately equiaxed ones. The average grain size of 252.6 ± 2 μm was obtained in the homogenized sample. The transformation of the dendritic microstructure into equiaxed after the homogenization process was also reported in the Al-2014 and Al-6061 alloys.[24–26]

Figure 2(a) shows the bright field TEM photomicrograph of the as-cast Al–Cu alloy sample after the HPT process. The microstructure consists of a combination of elongated (along the shear strained direction) and equiaxed grains with higher percentage of the elongated one. Similar observation of the formation of the elongated microstructure along the strain direction was also noted in the HPT processed Al-2024 alloy at room temperature.[22] The average grain size after the HPT of the as-cast Al–Cu alloy sample decreased to approximately 125 nm. The decrease of the grain size can be attributed to the imposed severe straining during the HPT process. The average grain size of the present HPT-processed as-cast Al–Cu alloy sample was very close to the reported average grain sizes (70 and 100 nm) in the HPT processed Al-2024 and Al-3%Cu alloys, respectively.[22,27] The SAED pattern of the HPT-processed as-cast Al–Cu alloy sample shown in Fig. 2 indicates the presence of low misorientation angle grain boundaries (LAGBs).

Figure 3(a) is the SEM photomicrograph exhibiting the θ phase ($CuAl_2$) in the as-cast Al–Cu alloy sample after the HPT process. It was reported that the hard θ phase particles after ECAP were fragmented across the sample: from the 5 μm to an average particle size of 600 nm.[17,20] Figure 4 shows the EDS spectrum analysis of the θ phase in the as-cast sample after the HPT process. The table in Fig. 4 indicates that the ratio of Al and Cu are very close to the exact mass composition of $CuAl_2$[28,29] and θ phase by EDS in previous work.[30] Moreover, the presence of the θ phase after the HPT process is in agreement with the detection of the θ phase

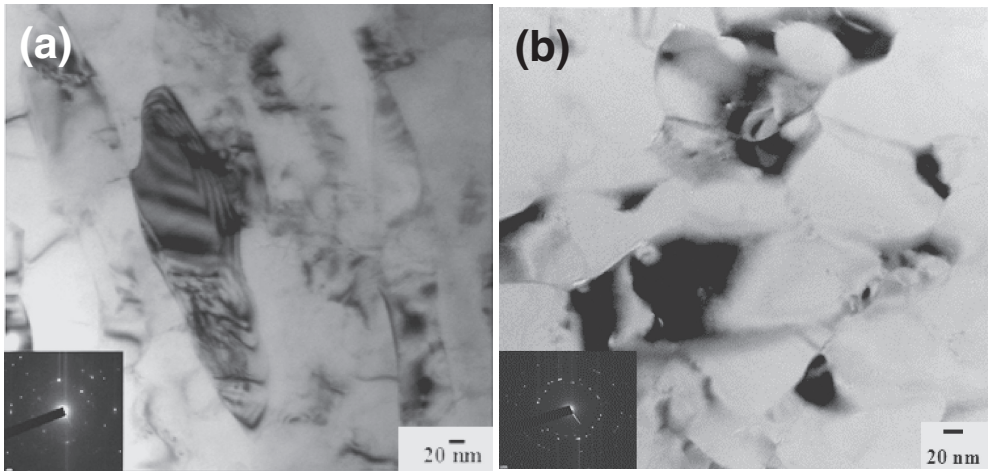

Fig. 2 TEM bright-field micrographs of (a) the as-cast Al-3%Cu alloy sample and (b) the homogenized Al-3%Cu sample after the HPT process.

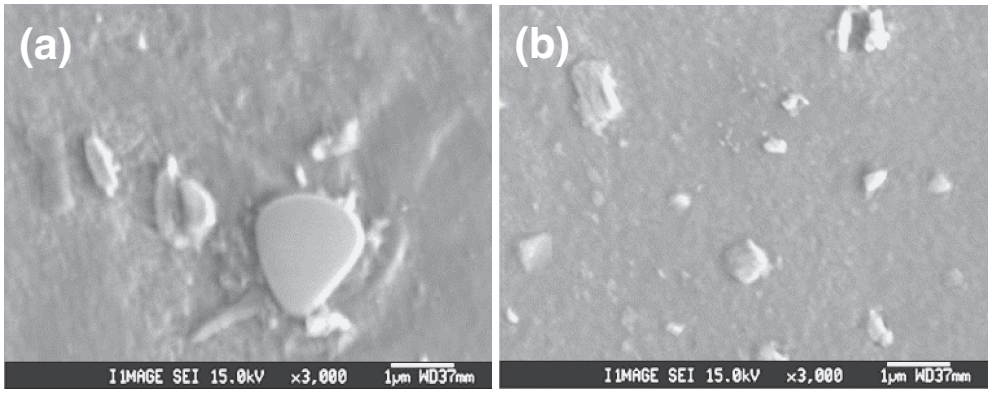

Fig. 3 FE-SEM micrograph of the θ phase particles in the (a) as-cast and (b) homogenized Al-3%Cu alloy samples after the HPT process.

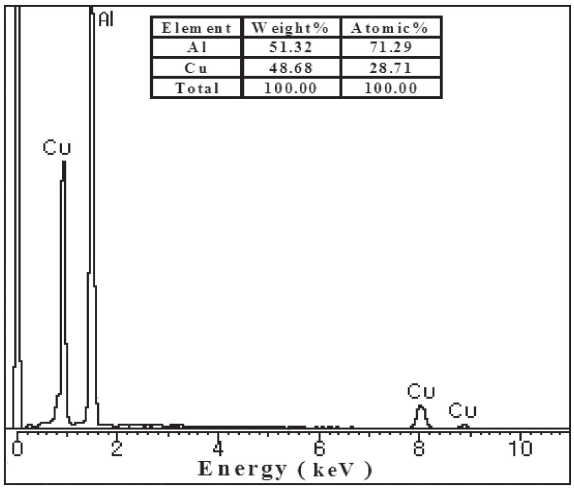

Element	Weight%	Atomic%
Al	51.32	71.29
Cu	48.68	28.71
Total	100.00	100.00

Fig. 4 EDS analysis of the θ phase ($CuAl_2$) in the as-cast Al–3%Cu alloy sample after the HPT process.

without any dissolution after the ECAP process of different Al–Cu alloys.[15,31] It was observed that θ phase particles almost did not re-dissolve up to 12 ECAP passes, on the other hand, the other phases (θ' and θ'' phases) were re-dissolved after 4 passes.[31] Moreover, the formation of the different precipitates in Al–Cu alloys depends mainly on the temperature at which the type of the precipitates formed. Therefore, we can confirm that the precipitate observed in the present work was θ phase.

It was observed that the θ phase particles agglomerated across the sample. That is, the θ phase particle distribution in the HPT-processed as-cast Al–Cu alloy sample is non-uniform. Similar observations of the fragmentation of the hard phases were noted in the ECAP-processed Al–Cu and Al-6061 alloys.[15,20,21,25,26] Figure 5(a) exhibits the size distribution of the θ phase particles of the HPT-processed as-cast sample. Approximately 65% of the particles are under 0.5 μm with a wide range of particle size from 0.2 to 1.4 μm. The average θ phase particle size is 600 nm after the HPT process, which is a half of that after the ECAP with 6 passes of the same alloy.[20] Figure 5(b) exhibits the θ phase particle distribution of the homogenized Al–Cu alloy after the HPT process. Approximately 76% of the particles are under 0.5 μm in size with a range of particle size from 0.08 to 0.9 μm which is narrower with smaller particle sizes than that observed in the HPT-processed as-cast sample, as shown in Fig. 5(a).

Figure 2(b) shows the bright field TEM photomicrograph after the HPT process of the homogenized Al–Cu alloy sample. The homogenized Al–Cu alloy sample after HPT consists of equiaxed grains with an average grain size of 65 nm. The average grain size observed after the HPT of the homogenized Al–Cu alloy sample was 48% smaller than that

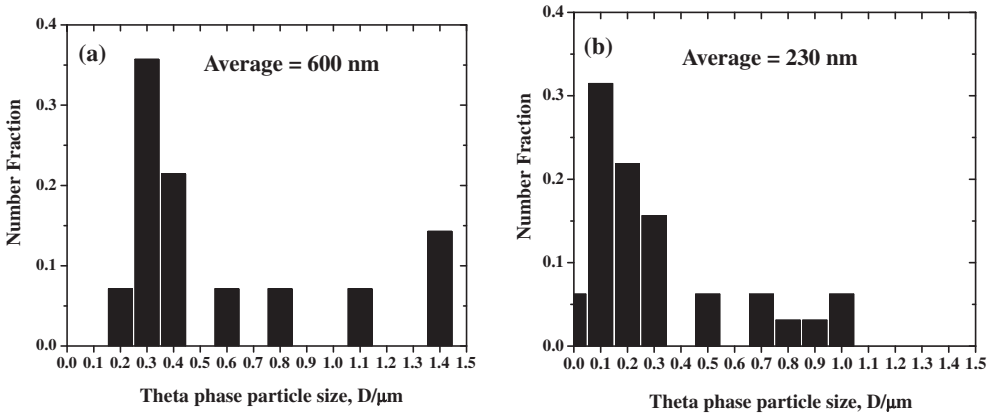

Fig. 5 Particle size distributions of the θ phase in the (a) as-cast and (b) homogenized Al-3%Cu alloy samples after the HPT process.

after the HPT process of the as-cast Al–Cu alloy. Similar observations were also noted during the ECAP of the as-cast and homogenized Al-2 and 3% Cu alloys samples.[20] The average grain size obtained in the ECAP-processed homogenized Al-3% Cu alloy sample was 25% smaller than that observed in the ECAP-processed as-cast Al-3% Cu alloy sample. Hence, it is clear that the homogenization treatment contributes to further degrees of grain refinement in the HPT and ECAP processes. The comparison between the HPT-processed and ECAP-processed Al–Cu alloy samples indicates that the average grain sizes of the HPT-processed as-cast and homogenized samples were 20 and 44%, respectively, smaller than those observed in the ECAP-processed samples.[20] The smaller average grain sizes of the Al matrix in the HPT-processed samples can be attributed to the higher strain and pressure imposed during the HPT process than those imposed in the ECAP process.[1–3] The SAED pattern after the HPT process of the homogenized Al–Cu alloy sample shown in Fig. 2(b) indicates the presence of high misorientation angle grain boundaries (HAGBs).

Figure 3(b) shows the SEM photomicrograph of the distribution of the hard θ phase ($CuAl_2$) after the HPT process of the homogenized Al–Cu alloy sample. It was observed that the hard θ phase particles were fragmented and uniformly distributed across the sample. Figure 5(b) shows the θ phase particles distribution of the homogenized Al–Cu alloy after the HPT process. Approximately 76% of the particles are under 0.5 μm with a range of particle size from 0.08 to 0.9 μm, which is narrower with smaller particles than that in the HPT-processed as-cast shown in Fig. 5(a). The average particle size of the hard θ phase in the HPT-processed homogenized Al–Cu alloy sample was 228 nm, which is 160% smaller than that of the HPT-processed as-cast Al–Cu alloy sample. The average particle sizes of the hard θ phase after the HPT process in the as-cast and the homogenized Al–Cu alloy samples were 100% smaller than those observed in the ECAP-processed counterparts.[20] This can be attributed to the higher stain imposed during the HPT process than that during the ECAP process.[1–3]

3.2 Microhardness

Figures 6(a) to 6(d) show the color-coded maps of the microhardness distribution in the (a) as-cast, (b) homogenized, (c) HPT-processed as-cast, and (d) HPT-processed homogenized Al–Cu alloy samples. The microhardness distribution in the as-cast Al–Cu alloy sample was almost homogeneous (ranging between 95 and 125 Hv) across the sample area, as shown in Fig. 6(a). The average microhardness and standard deviation values indicated by the error bar (inhomogeneity index) in the as-cast sample were 116 ± 1.7 and 7 Hv, respectively, as shown in Fig. 8. After the homogenization process of the as-cast sample, the microhardness distribution becomes more uniform (ranging between 103 and 116 Hv), as shown in Fig. 6(b). The average microhardness and standard deviation values were 111 ± 0.3 and 2.5 Hv, respectively (Fig. 7). The inhomogeneity index decreases remarkably (by 180%) after the homogenization heat treatment. The decrease of the average microhardness after the homogenization treatment can be attributed to the increase of the grain size from 113 ± 2 to 252.6 ± 2 μm. On the other hand, the increase of the microhardness homogeneity after the homogenization is due to the transformation of the microstructure from dendrite microstructure in the as-cast sample to equiaxed microstructure.[20]

Figure 6(c) shows the microhardness distribution after the HPT process of the as-cast Al–Cu alloy sample. A low microhardness (90–110 Hv) region of a diameter of 1 mm in the center was observed. This microhardness value in the center of the HPT-processes sample is close to that in the center of the as-cast sample. The microhardness increased with increasing the distance from the center. There are also low microhardness regions distributed randomly across the sample in Fig. 6(c). That is, the microhardness distribution across the HPT-processed as-cast Al–Cu alloy sample is nonuniform. The average microhardness and standard deviation values in the HPT-processed as-cast Al–Cu alloy sample were 175 ± 1.4 and 16.5 Hv, respectively (Fig. 7). The microhardness increased by 50% after HPT in the as-cast Al–Cu alloy sample.

The microhardness distribution color-coded map after the HPT process of the homogenized Al–Cu alloy sample is presented in Fig. 6(d). A low microhardness (230–250 Hv) area with an average diameter of 1.1 mm in the sample center was detected. The microhardness values in the center were 125% higher than those of the homogenized sample. It was

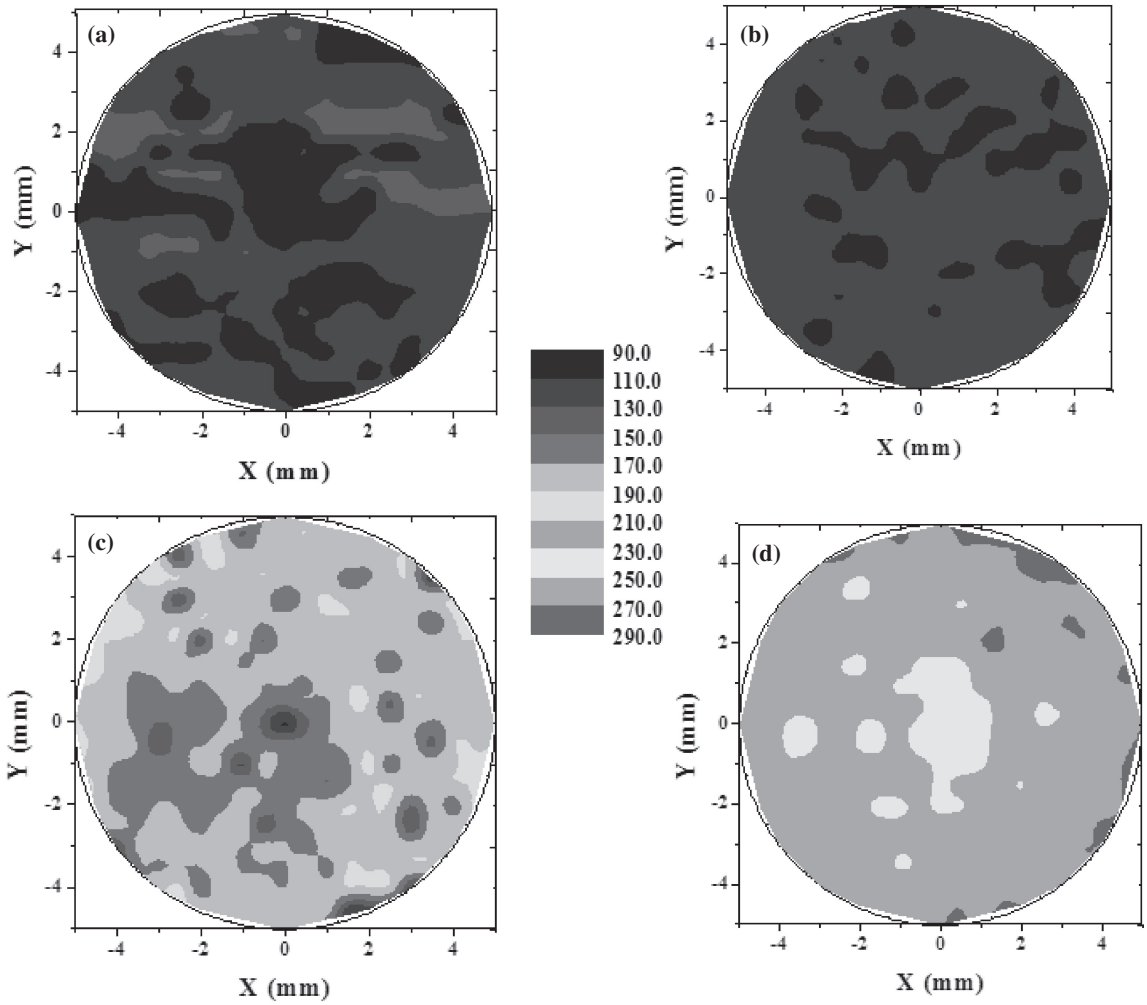

Fig. 6 Color-coded hardness contour maps showing the microhardness distribution across the surface of the (a) as-cast, (b) homogenized, (c) HPT processed as-cast and (d) HPT processed homogenized Al-3%Cu alloy samples.

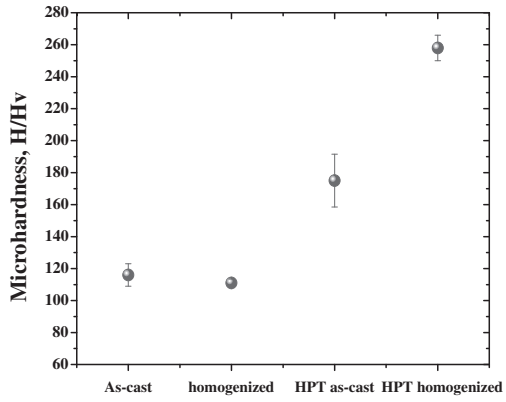

Fig. 7 Average microhardness and standard deviations (error bar) of as-cast, homogenized, HPT processed as-cast and HPT processed homogenized Al-3%Cu alloy samples.

also noted that the sample center of the homogenized sample deformed more than that in the as-cast one, as shown in Figs. 6(c) and 6(d). Microhardness increased with increasing the distance from the center and reaches 270–290 Hv near the sample edge. Approximately 80% of the sample area has the microhardness values of 250–270 Hv. The difference in the microhardness values between the sample center and edge is due to the difference in the imposed strain along the sample radius. Similar observations of the increased microhardness from the sample center to the edge were also noted in the various HPT-processed materials.[3,22,32] The average microhardness and the standard deviation value of the HPT-processed homogenized sample were 258 ± 1 and 8 Hv, respectively (Fig. 7). The microhardness increased by 133% after the HPT process of the homogenized Al–Cu alloy sample. The increase of the average microhardness after the HPT process of the as-cast and homogenized samples are attributed to the decreased Al matrix grain sizes and θ phase particle sizes. The hardness of a material is generally related to the grain size through a Hall–Petch equation.[33,34]

$$\mathrm{Hv} = H_0 + k_{\mathrm{H}} d^{1/2}, \tag{2}$$

where d is the grain size and H_0 and k_{H} are constants. In addition to the grain size effect, the increased of the dislocation density can also be considered as the reason for the increased strength after HPT, following the Taylor equation.[35]

$$\sigma = \sigma_0 + \alpha M G b \rho^{1/2}, \tag{3}$$

where α is a constant, G the shear modulus, b the length of the Burgers vector of dislocation, M the Taylor factor, and ρ dislocation density.

The average microhardness in the HPT-processed homogenized sample was 47% higher than that in the HPT-processed as-cast sample. This difference in the microhardness values can be attributed to (i) the smaller average grain size and (ii) the smaller θ phase particle size with more uniform distribution in the HPT-processed homogenize sample than that in the HPT-processed as-cast sample, as shown in Figs. 2, 3, and 5. The average microhardness values in the HPT processed as-cast and homogenized Al–Cu alloy samples were 20 and 35% higher than those obtained after the ECAP processes of the same samples, respectively.[20] This is due to the smaller grain size in the HPT-processed samples than in the ECAP-processed samples. However, the deformation homogeneity in terms of the microhardness distribution was higher in the ECAP-processed samples than that in the HPT-processed samples. Similar observations of higher degree of microhardness homogeneity in the ECAP-processed sample compared to that in the HPT-processed sample were also noted in Al-1080.[36] It was observed that the HPT-processed homogenized sample has more uniform distribution of the microhardness than that in the as-cast sample after the HPT process in Fig. 6. The inhomogeneity index in the HPT-processed as-cast sample is double the homogenized sample (Fig. 7). The average microhardness value in the HPT-processed homogenized Al–Cu alloy sample was 26% higher and more uniform than that in the Al-2024 alloy aged after the HPT process.[22]

3.3 Tensile testing

True stress vs. true strain curves of the Al–Cu alloys (as-cast, homogenized, and their HPT-processed samples) are shown in Fig. 8. The ultimate tensile strength (UTS) increased from 156.9 MPa in the as-cast sample to 520.5 MPa after the HPT process. The 0.2% proof stress significantly increased from 100.2 MPa in the as-cast sample to 425 MPa after the HPT process, which is 324% increase in strength.

In the homogenized Al–Cu alloy sample, the UTS increased by 335% from 146 to 636 MPa after the HPT process. A similar ratio increase was also observed in the 0.2% proof strength: from 95 to 510 MPa after the HPT process. The increase of the UTS and the 0.2% proof strength after the HPT process can be attributed to the decrease of the grain size, the fragmentation of the θ phase, and the increase of the dislocation density. Similar observations of the increase of the UTS and proof strength were also noted after the SPD processes of various Al–Cu alloys.[15,16,20]

The UTS and the 0.2% proof strength after the HPT process of the homogenized sample were 23 and 20% higher than those after the HPT process of the as-cast sample. The higher values of UTS and 0.2% proof strength in the HPT-processed homogenized sample is due to the finer grain and θ phase particle sizes and the homogeneous distribution of the θ phase. Similar observations were also reported in the ECAP-processed Al-2 and 3%Cu alloys. The UTS and the 0.2% proof strength after the ECAP process of the homogenized samples were 42 and 31%, respectively, higher than those obtained after the ECAP process of the as-cast samples.[20]

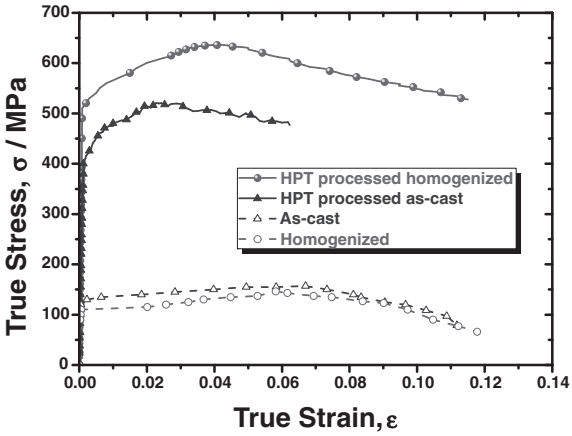

Fig. 8 True stress true strain relation of as-cast, homogenized, HPT processed as-cast, HPT processed homogenized Al-3%Cu alloy samples.

The UTS and the 0.2% proof strength of the HPT-processed Al–Cu alloy samples were 63 and 55%, respectively, higher than those obtained after the ECAP process of the same alloy.[20] This is due to the smaller Al matrix grain and θ phase particle sizes in the HPT-processed samples. Similar observations of higher UTS and yield strength in the HPT-processed samples than those of the ECAP-processed ones were also noted in the Al, Ti, and Cu.[36–38]

The elongation increased by 6% after the homogenization treatment as shown in Fig. 8. This is due to the microstructural transformation from the dendritic to equiaxed grain microstructures.[20] After the HPT process the elongation decreased from 11.2% in the as-cast sample to 6.2%. On the other hand, the elongation decreased slightly from 11.8 to 11.5% after the HPT process of the homogenized Al-3%Cu alloy sample, which is 86% higher than that of the HPT processed as-cast sample.

Higher elongation after the HPT process of the homogenized sample results from the presence of HAGBs, as shown in the SAED in Fig. 2(b). The fine precipitates lead to HAGBs in the deformation zones surrounding the particles.[1] Moreover, as the size of the secondary phase decreases, the inhibition of the dislocation movement decreases. Similar observations of increased elongation in the homogenized samples over as-received samples were also reported after the ECAP process of the Al-2 and 3% Cu samples.[20] This was also noted through the study of the effect of pre-heat treatment on the degree of the grain refinement and tensile properties during the ECAP and cryogenic rolling process of Al-7034 and Al-6063 alloys.[39,40] The elongation values of the HPT-processed Al–Cu alloys of the as-cast and homogenized samples were higher than those of the ECAP-processed samples.[20] The elongation in the HPT-processed as-cast and homogenized samples were higher by 24 and 39% than those in the ECAP-processed samples, respectively.[20] Similar observations were also noted through the ECAP and HPT processes of Al and Cu.[36,38] The elongation values of the HPT-processed Cu and Al samples were higher by 56 and 17% than those in the ECAP-processed Cu and Al samples, respectively.[36,38]

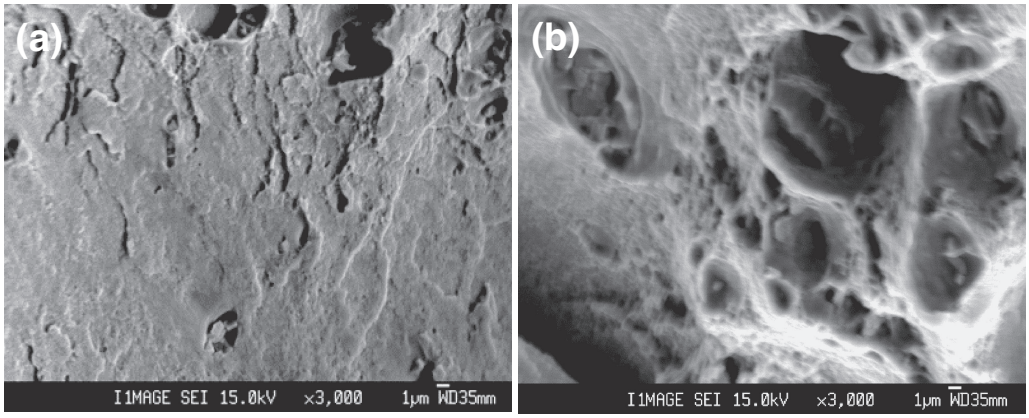

Fig. 9 FE-SEM micrograph of the tensile fracture surface morphology of HPT-processed (a) as-cast and (b) homogenized Al-3%Cu alloy samples.

3.4 Fracture behavior

The tensile fracture surface morphology of the as-cast Al–Cu alloy was fully investigated in previous work.[21] It was observed that the fracture surface consists of a dendrite structure with inter-dendritic micro-porosities, which is a typical casting defect. The presence of the dendritic structure and micro-porosity was also observed on the fracture surfaces of the as-cast Al-4%Cu, Al-40%Zn, and Zn-40%Al alloys.[16,41,42]

Figure 9 shows the FE-SEM photomicrographs of the fracture surface morphologies of the HPT-processed (a) as-cast and (b) homogenized samples. In the HPT-processed as-cast sample, the dendritic structure was almost eliminated from the fracture surface, as shown in Fig. 9(a). The fracture surface consists of a shear decohesion feature, lacking any appearance of dimples. This can be attributed to the grain refinement by the HPT process. Moreover, fractured particles and delamination zones were also observed through the fracture surface. These observations are in agreement with the result of the elongation (i.e., the elongation decreased remarkably by 44.7% after HPT) shown in Fig. 8. Similar observations of the elimination of the dendritic structure and the micro-porosity of the fracture surface were also found after the ECAP process of Al-4%Cu, Al-2 and 3%Cu, Al-40%Zn, and Zn-40% Al alloys.[16,21,41,42] After the homogenization treatment, the fracture surface morphology was free from the dendritic structure[18,21] due to the transformation of the microstructure to equiaxed one.

Figure 9(b) shows the FE-SEM photomicrograph of the fracture surface morphology of the HPT-processed homogenized sample. Large, deep, and uniformly distributed dimples appeared with the size range of 0.1–13.5 μm and an average size of 1.9 μm. The presence of the dimples on the fracture surface indicates the occurrence of ductile fracture. This result is in agreement with the tensile elongation results that the HPT-processed homogenized sample has twice the ductility than that of the HPT-processed as-cast sample as shown in Fig. 8.

The difference in initial microstructure of the as-cast and homogenized samples obviously affects the microstructure evolution of the HPT-processed samples, as shown in Figs. 2–5. It was clearly noted that the HPT-processed homogenized samples have equiaxed grains with HAGBs, while HPT-processed as-cast samples have elongated grains with LAGBs. This difference in the microstructure in both materials leads to obvious difference in their ductility, as shown in Fig. 8. Further comparison indicates that the HPT-processed homogenized samples have ductility nearly double the value of the HPT-processed as-cast sample. Moreover, the ductility of the homogenized sample slightly decreased after the HPT process. The HPT-processed homogenized samples is ductile and consistent with the fracture surface covered by dimples, as shown in Fig. 9(b). On the other hand, the ductility of the as-cast sample decreased remarkably after the HPT process by 44.7%, indicating that the HPT-processed as-cast sample lost its ductility and the fracture surface consists of a shear decohesion feature, as shown in Fig. 9(a).

Similar observation of the effect of the pre-homogenization treatment on the fracture surface morphology was also noted after the ECAP process of the Al-2 and 3% Cu alloys.[21] The shear decohesion, fractured particles, and delamination zones on the fracture surface of the ECAP-processed as-cast samples exhibit obviously different features from the dimples in ECAP-processed homogenized samples.[21]

Figure 10(a) shows the fracture surface of the HPT-processed as-cast sample, indicating the shear mode after HPT, in contrast to the brittle fracture before HPT.[21] There was no obvious reduction of the cross-sectional area of the fractured specimen after the HPT process of the as-cast sample. In the HPT-processed homogenized sample, the fracture mode was transformed from the brittle fracture before HPT[21] to a combination of shear and necking (ductile) fracture mode after the HPT process, as shown in Fig. 10(b). A clear reduction in the cross-sectional area of the fractured sample was observed in the HPT-processed homogenized sample, as indicated by the arrows in Fig. 10(b). The area reduction in the HPT-processed homogenized sample was 14%, which is close to the elongation value obtained through the tensile test, as shown in Fig. 8. The difference in the fracture mode between the HPT-processed as-cast and homogenized samples is another piece of evidence that the HPT-processed homogenized samples have higher ductility than that in the HPT-processed as-cast samples.

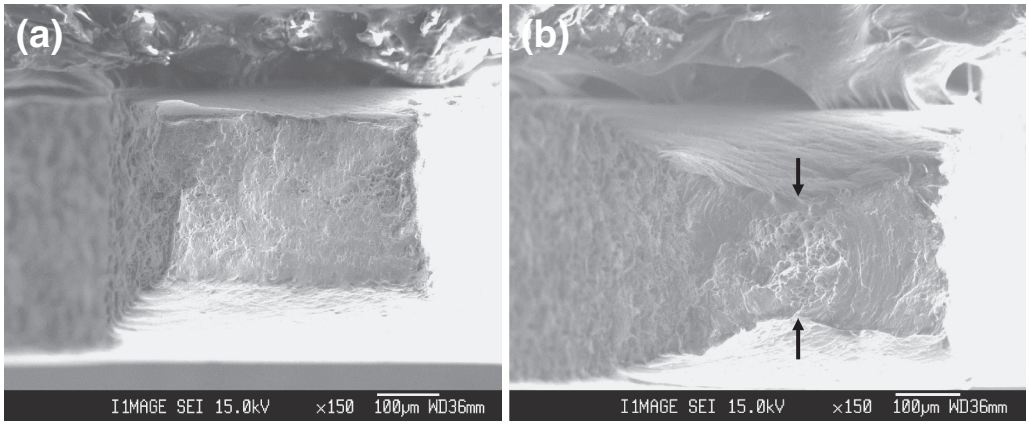

Fig. 10 FE-SEM micrograph of the tensile fracture shapes of HPT-processed (a) as-cast and (b) homogenized Al-3%Cu alloy samples.

4. Conclusions

Through the investigation of the effect of the pre-homogenization treatment on the microstructure evolution, mechanical properties, and fracture characteristics of the HPT-processed Al–Cu alloy, the following conclusions were drawn:

(1) The pre-homogenization process helps in the evolution of the microstructure into equiaxed UFG microstructures with high misorientation angle grain boundaries and the average grain size of 65 nm after HPT. On the other hand, elongated grains with low misorientation angle grain boundaries and the average grain size of 125 nm microstructure were obtained in the HPT-processed as-cast sample.

(2) An obvious decrease in average grain size to 228 nm with more homogenous distribution of the θ phase was observed in the HPT-processed homogenized sample.

(3) A remarkable increase in the microhardness was observed after the HPT process of the as-cast and homogenized samples. The average microhardness value in the HPT-processed homogenized sample was higher than that of the HPT-processed as-cast sample. Higher deformation homogeneity was obtained in the HPT-processed homogenized sample than that in the HPT-processed as-cast sample.

(4) The strength increased after the HPT process of the as-cast and homogenized samples while the elongation decreased.

(5) The fracture surface morphologies exhibited shear decohesion, fractured particles, and delamination in the HPT-processed as-cast sample and ductile fracture surface covered with dimples in the HPT-processed homogenized sample.

(6) The fracture mode were transformed from the brittle mode before HPT to the shear mode and the combination of shear and necking (ductile) modes after HPT in the as-cast and homogenized samples, respectively.

Acknowledgements

This work was supported by grant No. KSC-2012-C2-09 from Korea Institute of Science and Technology Information. HYU and KHC are supported by the BK+ program.

REFERENCES

1) R. Z. Valiev, R. K. Islamgalive and I. V. Alexandrov: Prog. Mater. Sci. **45** (2000) 103.
2) R. Z. Valiev and T. G. Langdon: Prog. Mater. Sci. **51** (2006) 881.
3) A. P. Zhilyaev and T. G. Langdon: Prog. Mater. Sci. **53** (2008) 893.
4) H. S. Kim, S.-H. Joo and H. J. Jeong: Korean J. Met. Mater. **52** (2014) 87.
5) W. Wang, Y. Song, D. Gao, E. Y. Yoon, D. J. Lee, C. S. Lee and H. S. Kim: Met. Mater. Int. **19** (2013) 1021.
6) E. Y. Yoon, D. J. Lee, B. Park, M. R. Akbarpour, M. Farvizi and H. S. Kim: Met. Mater. Int. **19** (2013) 917.
7) K. H. Lee and S. I. Hong: Korean J. Met. Mater. **51** (2013) 621.
8) S.-H. Lee and J.-H. Kim: Korean J. Met. Mater. **51** (2013) 251.
9) E. Çadirl: Met. Mater. Int. **19** (2013) 411.
10) H. K. Moon, J. Yoon, H. Kim and N.-E. Lee: Met. Mater. Int. **19** (2013) 611.
11) C. H. Jeon, S. W. Han, B. D. Joo, C. J. Van Tyne and Y. H. Moon: Met. Mater. Int. **19** (2013) 1069.
12) K. S. Lee, S. E. Lee, J. S. Kim, M. J. Kim, D. H. Bae and Y.-N. Kwon: Korean J. Met. Mater. **51** (2013) 535.
13) S. Lee, J.-S. Lee, Y.-B. Kim, G.-A. Lee, S.-P. Lee, I.-S. Son, J.-K. Lee and D.-S. Bae: Korean J. Met. Mater. **51** (2013) 655.
14) M. Murayama, Z. Horita and K. Hono: Acta Mater. **49** (2001) 21.
15) D. R. Fang, Z. F. Zhang, S. D. Wu, C. X. Huanga, H. Zhang and N. Q. Zha: Mater. Sci. Eng. A **426** (2006) 305.
16) E. Prados, V. Sordi and M. Ferrante: Mater. Sci. Eng. A **503** (2009) 68.
17) N. El Mahallawy, F. A. Shehata, M. A. El Hameed and M. I. Abd El Aa: Mater. Sci. Eng. A **517** (2009) 46.
18) M. I. Abd El Aal, N. El Mahallawy, F. A. Shehata, M. A. El Hameed, E. Y. Yoon, J. H. Lee and H. S. Kim: Met. Mater. Int. **16** (2010) 709.
19) M. I. Abd El Aal, N. El Mahallawy, F. A. Shehata, M. A. El Hameed, E. Y. Yoon and H. S. Kim: Mater. Sci. Eng. A **528** (2011) 6946.
20) M. I. Abd El Aal: Mater. Sci. Eng. A **527** (2010) 3726.
21) M. I. Abd El Aal: Mater. Sci. Eng. A **539** (2012) 308.
22) R. Vafaei, M. R. Toroghinejad and R. Pippan: Mater. Sci. Eng. A **536** (2012) 73.
23) C. Xu, M. Furukawa, Z. Horita and T. G. Langdon: Mater. Sci. Eng. A **398** (2005) 66.
24) C. Mallikarjuna, S. M. Shashidhara and U. S. Mallik: Mater. Des. **30** (2009) 1638.
25) C.-Y. Chou, S.-L. Lee and J.-C. Lin: Mater. Sci. Eng. A **485** (2008) 461.
26) M. W. Fu, Y. W. Tham, H. H. Hng and K. B. Lim: Mater. Sci. Eng. A **526** (2009) 84.
27) P. Parz, M. Faller, R. Pippan, H. Reingruber, W. Puff and R. Würschum: J. Appl. Phys. **112** (2012) 103506.

28) http://www.webqc.org/mmcalc.php.
29) J.-G. Jung, J.-S. Park and Y.-K. Lee: Met. Mater. Int. **19** (2013) 147.
30) T. H. Lee, J. H. Sun, H. H. Nersisyan, H. G. Jung, K. H. Lee and J. H. Lee: Composites Part A **43** (2012) 1490.
31) X. U. X. Chang, L. Z. Yi, L. Y. Tao, D. Peng and Z. S. Min: Trans. Nonferrous Met. Soc. China **18** (2008) 1047.
32) K. Edalati and Z. Horita: Mater. Trans. **51** (2010) 1051.
33) M. E. O. Hall: Proc. R. Soc. B **64** (1951) 747.
34) N. J. Petch: J. Iron Steel Inst. **174** (1953) 25.
35) G. I. Taylor: Proc. R. Soc. A **145** (1934) 362.
36) M. I. Abd El Aal, E. Y. Yoon and H. S. Kim: Metall. Mat. Trans. A **44** (2013) 2581.
37) A. V. Sergueeva, V. V. Stolyarov, R. Z. Valiev and A. K. Mukherjee: Scr. Mater. **45** (2001) 747.
38) N. Lugo, N. Llorca, J. M. Cabrera and Z. Horita: Mater. Sci. Eng. A **477** (2008) 366.
39) C. Xu, M. Furukawa, Z. Horita and T. G. Langdon: Acta Mater. **51** (2003) 6139.
40) S. K. Panigrahi, R. Jayaganthan and V. Pancholi: Mater. Des. **30** (2009) 1894.
41) O. Saray and G. Purcek: J. Mater. Proc. Technol. **209** (2009) 2488.
42) G. Purcek, O. Saray, I. Karaman and T. Kucukomeroglu: Mater. Sci. Eng. A **490** (2008) 403.